Journal of Hydrology 596 (2021) 125699

Contents lists available at ScienceDirect

Journal of Hydrology

journal homepage: www.elsevier.com/locate/jhydrol

Research papers

Linking nitrate dynamics to water age in underground conduit flows in a karst catchment

Zhicai Zhang [a,*], Xi Chen [b], Siliang Li [b], Fujun Yue [b], Qinbo Cheng [a], Tao Peng [c], Chris Soulsby [d]

[a] College of Hydrology and Water Resources, Hohai University, Nanjing 210098, China
[b] Institute of Surface-Earth System Science, Tianjin University, Tianjin 300072, China
[c] Institute of Geochemistry, Chinese Academy of Sciences, Guiyang 550081, China
[d] School of Geosciences, University of Aberdeen, Aberdeen AB24 3UF, United Kingdom

ARTICLE INFO

This manuscript was handled by Corrado Corradini, Editor-in-Chief

Keywords:
Karst catchment
Nitrate dynamics
Water age
Underground conduit

ABSTRACT

Although numerous studies on nitrate transport and transformation in karst catchments have been reported, many challenges in understanding nitrate fluxes remain due to the unique architecture of karst critical zones and complex hydrological processes. Water age is an important descriptor of hydrological function providing insight to into flow paths and water sources at the catchment scale. This offers a potential opportunity to better understand the spatio-temporal variations in nitrate dynamics in karst catchments. We linked the nitrate dynamics of underground conduit flow to water age extracted from a robust tracer-aided model for a karst catchment in southwestern China. The results show that nitrate dynamics in underground conduit flow are controlled by the coupling of nitrate supply and of flow paths in the karst catchment. High contributions of drainage from small fractures water leads to low nitrate concentrations in underground conduit flow during the dry season. This reveals that the small fractures may be another important "hot spot" for denitrification leading to nitrate removal in the karst critical zone. The switching between transport limited and supply limited conditions cause the marked variations in nitrate concentration of underground conduit flow during wet season. Although rapid infiltration via large fractures and sinkholes have strong dilution effects on nitrate in underground conduit flow at beginning of rainfall, more nitrate was transported out of the catchment with drainage during rainfall events due to the mobilization of soil nitrate by rainfall. Meanwhile, the capacity to transport nitrate out of catchment can be potentially activated when the 'old' water is displaced by rainfall under high wetness condition.

1. Introduction

The karst critical zone comprises complex porous media, encompassing soil, small fractures, large fractures, and conduits (Ford and Williams, 2007), which cause a diverse range of hydrological processes at the catchment scale (Hartmann et al., 2014). The sharp responses of stream and underground conduit flows to rainfall are notable due to the very high permeability of karst aquifers and well-developed subsurface fracture - conduit networks (White, 2002). In particular, the unique landform structure of sinkholes provides direct flow paths linking the surface/epikarst to underground drainage networks after heavy rain, which strengthens hydrological connectivity between surface and subsurface systems (Tihansky, 1999).

Increased fertilization using N for agriculture creates a high N pollution risk in karst (Maringanti et al., 2009; Yang et al., 2020). High nitrate concentrations in streamflow have been observed in many agricultural catchments with intense fertilization (Kellman and Hillaire-Marcel, 2003; Barnes and Raymond, 2009; Heaton et al., 2012). Over-application of fertilizer, as well as wrong timing of application, potentially lead to major nitrate leaching losses and unsustainable land and water management practices (Di and Cameron, 2002). Understanding the resulting spatio-temporal dynamics of nitrate in aquifer and stream flow is critical to water resources and agriculture management in karst areas. The transport and transformation of nitrate in karst areas is more complex than that in non-karst environments because of the marked spatial heterogeneity of the hydrodynamic behaviour (Hartmann et al., 2014). Along with water flows in the karst critical zone, nitrate transport is strongly controlled by hydrological connectivity between different landform units (e.g., hillslopes and depressions) as well as different porous media (e.g., small fractures and conduits) (Zhang et al., 2020a).

* Corresponding author.
E-mail address: zhangzhicai_0@hhu.edu.cn (Z. Zhang).

https://doi.org/10.1016/j.jhydrol.2020.125699

Available online 26 October 2020

Nitrate is easily leached into aquifers due to the thin soils and quick infiltration rate in karst (Yue et al., 2015). In addition to soil, the epikarst is a substantial nitrate reservoir where the transport and biogeochemical transformations of nitrate (e.g., denitrification) cannot be ignored (Husic et al., 2019). An important research gap on nitrate in karst regions is that different nitrate transport pathways affect nitrate behaviour in stream or underground conduit flows. Although some researchers have reported findings on this, results can be contradictory. For example, Husic et al. (2019) indicated that the slow to moderate flow pathways in epikarst contribute most nitrate to streamflow (nearly 90% of the downstream nitrate flux), while Wang et al. (2020) found that very large amounts of nitrate enter drainage systems through fast flow paths after heavy rains.

Characterisation of the relationship between nitrate concentration and discharge (C-Q) is a popular method for assessing nitrate dynamics at the catchment scale (Basu et al., 2010; Duncan et al 2017; Zhi et al., 2019). The C-Q response pattern is usually categorized into three types: dilution, enrichment, and constant, which imply different hydrological flow paths and biogeochemical reactions (Musolff et al., 2017). In particular, the C-Q relationship for a rainfall event usually exhibits looped trajectories due to hysteretic behaviour of the solute concentration relative to discharge (Williams, 1989). Analysis of the C-Q hysteresis behaviour has been widely adopted to examine solute transport in catchments (Bieroza and Heathwaite, 2015; Bowes et al., 2015; Lloyd et al., 2016; Perks et al., 2015). It can provide insights into the spatio-temporal dynamics of solute concentrations and their linkage to watershed structure, storage variations and hydrologic connectivity under different hydroclimatic conditions (Perks et al., 2015).

As descriptors of hydrological function, the age of water in various fluxes can reveal how catchment storage mediates flow path activation and mixing processes (Kirchner et al., 2000; Botter, 2012; McDonnell and Beven, 2014; Soulsby et al., 2015; Sprenger et al., 2019). Therefore, linking solute dynamics to water ages can potentially provide new insights into the coupling of hydrological and transport processes at the catchment scale (Benettin et al., 2015; 2020;; Tunaley et al., 2016). Metrics of water age are traditionally referred to as specific times, such as the mean travel time, defining as the average time interval between the entrance and the exit of a water particle in a catchment; or the mean residence time of water in a particular store; and the alternative age metrics of young water fraction, defining the fraction of water with transit times between zero and a specific age threshold (typically 2–3 months).

Water aged have been widely estimated using conservative tracers (e.g., stable isotopes) (Hrachowitz et al., 2009; Birkel and Soulsby, 2015; Kirchner, 2016a, 2016b). Time-invariant approaches (e.g., lumped convolution approaches) were often adopted in the early estimations of travel time distributions (TTD) and mean travel times (MTT), as well examination of the influences of climate and landscape properties (Heidbüchel et al. 2013). However, these simplified approaches have limited application in complex, dynamic flow systems exhibiting non-steady state response to hydroclimatic variability (Botter, 2012). Many time-variant approaches have been proposed for the characterization of age distributions of catchment water storage and fluxes. For example, water age dynamics can be inferred by simulating transport processes at the catchment scale through StorAge Selection (SAS) functions that collapse complex transport processes into a unified framework of age-related storage (Rinaldo et al., 2015). Recent advances in tracer-aided hydrological modelling have also provided more constrained water age estimates by tracking water and tracer fluxes (e.g., McMillan et al., 2012; Soulsby et al., 2015; Piovano et al., 2019). Moreover, tracer-aided models allow the estimation of probability density functions (pdfs) of travel/residence times describing the fate of rainfall water particles traveling through catchments (Remondi et al., 2018).

Despite many existing studies on nitrate dynamics and their controlling influences in karst areas (Liu et al., 2006; Schilling and Helmers, 2008; Husic et al., 2019), great challenges in improving understanding of nitrate transport and transformation in this unique hydrogeological system remain. To help address the general research gaps in nitrate processes in karst catchments, our overall objective is to use water ages as a tool to better understand the influence of flow path dynamics on nitrate behaviour in underground conduits and the associated controlling effects of hydroclimatic and nitrate supply conditions. More specifically, in this study, we address three questions for karst catchment: (1) What are the relationships between nitrate concentration/loading and water age in underground conduit flow under different hydroclimatic conditions? (2) How does the intra-rainfall event hysteresis between nitrate concentration and water age of underground conduit flow vary under different hydroclimatic conditions? (3) How do water sources and flow paths affect nitrate and water age dynamics in underground conduit flow?

2. Site and Methodology

2.1. Study catchment

The Chenqi catchment with surface area of 1.25 km^2, is a typical cockpit karst landscape located at the Puding Karst Ecohydrological Observation Station in Guizhou Province, Southwest China (Fig. 1). This catchment is surrounded by conical hills separated by star-shaped valleys (Zhang et al., 2011; Chen et al., 2018). The elevation ranges from 1,340 to 1,500 m above sea level (Fig. 1a). This region is subject to a subtropical wet monsoon climate and has a mean annual temperature of 20.1 °C, with the highest temperatures typically occurring in July and the lowest ones in January. The mean annual precipitation is 1,140 mm according to long-term measured data in the catchment. The wet season lasts from May to September and the dry season from October through to April of the following year. The catchment contains two main landscape units: depressions with low elevations (<1340 m) and hillslopes with a high elevation ranging from 1,340 ~ 1,500 m. The spatial extents of the depressions and hillslopes derived from a 1:10,000 digital topography map are 0.37 and 0.88 km^2, respectively. The catchment is drained by a single underground conduit (Fig. 1a).

Geological units in the catchment include dolostone, thick and thin limestones, marl and Quaternary soil. The thickness of the limestone formations is approximately 150–200 m above the impervious marl formation. The low permeability causes precipitation to recharge perched groundwater on the marl, which then moves laterally to be discharged in the lower areas. Hence, the marl formation is a key control on the distribution of hillside springs in this region. On the hillslopes, the Quaternary soils covering carbonate rocks are very thin with an average thickness of 30 cm, while the average thickness of the soil layer in the depression is greater than 2 m. Limestone fragments occur in the soil layer, and the rock outcrop area accounts for 10–30% of the total area. The vegetation characteristics include deciduous broad-leaved forests, shrubs and grass at the top and middle of the hillslopes and crops at the lower end of the hillslopes and in the depression, which has a thick soil layer (Fig. 1b). A rice-rape crop rotation is the main land use in the depression, and a corn-rape crop rotation occurs at the foot of the hillslopes. Fertilization is common in agricultural regions in southwest China, leading extensive, potentially long-term contamination of the karst system (Fenton et al., 2017). In this catchment, organic fertilizers (e.g. cattle and pig manure) and chemical fertilizers (e.g. urea and diammonium phosphate) are mainly applied for rice and rape crops in the depression (Fig. 1). The light fertilization for rape occurs in October-November, and the heavy fertilization for rice is in May-early June (Yue et al., 2019).

At Chenqi, there are two flow observation points, the underground conduit spring at catchment outlet and a hillslope spring located at the foot of the eastern steep hillslope (Fig. 1a). The discharge at the two springs is measured at time intervals of 15 min using v-notch weirs instrumented with HOBO U20 water level loggers (Onset Corporation, USA). Four automatic weather stations are located on the upper

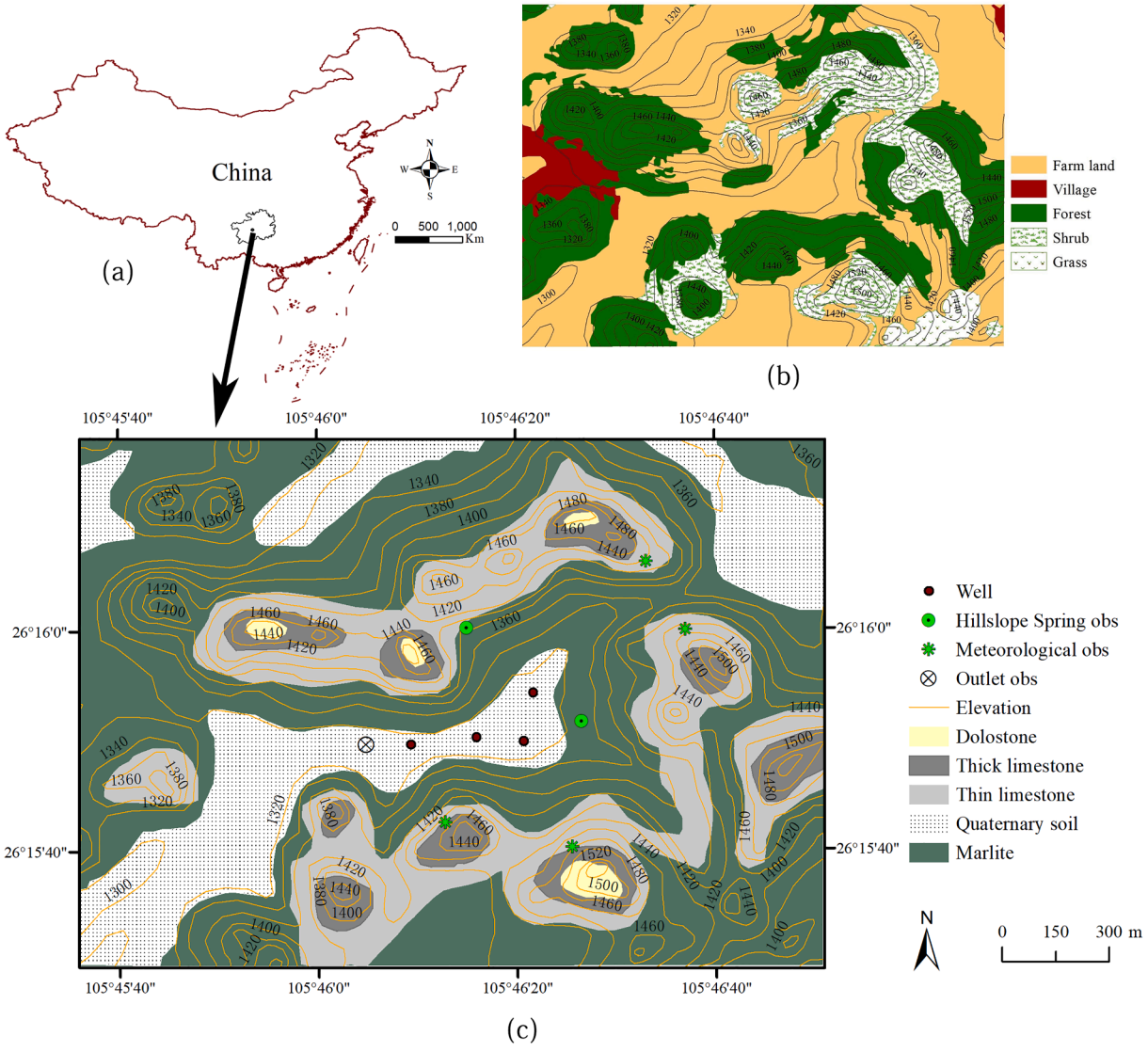

Fig. 1. Map of (a) the location, (b) vegetation, and (c) geology, geomorphology, hydrological monitoring locations in the Chenqi catchment. The village is outside the study catchment.

hillslopes. Precipitation, air temperature, wind parameters, radiation, air humidity and air pressure are all recorded at time intervals of 5 min. The NO_3-N concentration at the catchment outlet is monitored using a non-optical NISE sensor at time intervals of 15 min. The sensor is powered by 24 V DC batteries supplemented by solar panels. The sensor has been calibrated using the laboratory measured concentrations of grab samples manually collected over the duration of the observation period, and the uncertainty of estimated field NO_3-N is between 0.04 and 0.64 mg/L (Yue et al., 2019). All the observations were performed from 1 November 2016 to 30 October 2017.

2.2. Simulated age and travel time distribution of underground conduit flow

A tracer-aided hydrological model for karst catchments has been developed and applied to Chenqi by Zhang et al. (2019). This model disaggregates the cockpit karst catchment into the two dominant landscape units of the hillslopes and depressions. For depressions, a two-reservoir model (linking slow and fast reservoirs) is applied to simulate the water and tracer transport conceptualising the typical dual-flow system of the karst critical zone (Hartmann et al., 2014). The slow flow reservoir represents the low-permeability media, e.g., primary porosity in the matrix blocks and small fractures in the aquifer. The fast flow reservoir mainly represents the large fractures and conduits with a high permeability. The outlet of the fast flow reservoir is the catchment outlet. To reduce the model parameterization, one reservoir with an additional passive store only for the tracer mixing simulation is employed to estimate the water and tracer dynamics in the hillslope unit. This method can not only realize the partial mixing of tracers at the catchment scale, but can also reduce the model parameterization (Tetzlaff et al., 2014). Model calibration and verification have been performed using high-temporal resolution measured data (hourly) of flow and stable isotopes at outlet, hillslope spring and groundwater wells in the study catchment (full detail in Zhang et al., 2019). The results revealed that the model can capture the flow and tracer dynamics within each landscape unit quite well, and has a strong capacity to track the hourly water and isotope fluxes through each landscape unit. This allows the associated storage and hydrological connectivity dynamics to be characterised, as well as the time-variant age of underground conduit flow (Zhang et al., 2019). The series of flow age over the study period derived from this tracer-aided model were used to explore nitrate export from the catchment by linking it to observed nitrate dynamics.

Furthermore, once calibrated, the tracer-aided model can be run multiple times in parallel to separately track the fate of each hourly

rainfall input during event. The water over each rainfall hour is uniquely labelled with a specific tracer concentration. Then, by estimating the variation in tracer mass over time at the catchment outlet, the fate of the rainwater during each rainfall hour (reaching the outlet as discharge) can be tracked forward. Hence, the travel time distributions (TTD) of rain entering catchment at each rainfall hour can be estimated (Remondi et al., 2018). Then, the discharge over time at outlet generated by a specific rainfall can be calculated by multiplying the corresponding water amount of rainfall minus evaporation and its TTD. Using this approach, a total of 892 rainfall hours during the study period were tracked, and the results were used to explore the dynamics of nitrate export at catchment outlet driven by rainfall. The amount of NO_3-N export depends on the NO_3-N concentration and discharge at underground conduit outlet. For each time step, the NO_3-N export driven by a specific rainfall is calculated by the NO_3-N concentration of underground conduit flow multiplied by the discharge generated from the corresponding rainfall (i.e. the amount of rainfall minus evaporation multiplied by TTD of outflow). This means that, based on the observed concentrations, the estimation of NO_3-N export over time driven by each rainfall event only takes into account the discharge generated by it, without considering the biogeochemical reactions.

Please refer to Zhang et al. (2019) and Zhang et al. (2020b) for full details on how the flow age was calculated and how rainwater was tracked in the model.

2.3. Hysteresis analysis

As a fingerprint of water flow, water age is usually treated as a specific tracer "concentration" (Botter et al., 2011; Remondi et al., 2018). Similar to the relationship between concentration and discharge (C-Q), the relationship between water age and discharge (A-Q) is a potential descriptor providing information about flow paths and mixing processes. In this study, the hysteretic behaviour of nitrate and water age were estimated with the method of the loop cyclic of C-Q and A-Q, respectively, which reveal the lags in response between discharge and solute concentration and water age. The hysteresis index by Lloyd et al., (2016) is adopted to characterize the size and shape of the hysteresis loop. First, raw discharge and concentration data for individual rainfall events are normalized by:

$$Q_i = \frac{Q_i - Q_{min}}{Q_{max} - Q_{min}} \quad (1)$$

$$C_i = \frac{C_i - C_{min}}{C_{max} - C_{min}} \quad (2)$$

where Q_i and C_i are the discharge and concentration, respectively, at time step i; Q_{min} and C_{min} are the minimum discharge and concentration, respectively; Q_{max} and C_{max} are the maximum discharge and concentration, respectively. Based on the normalized data, the hysteresis index at a specific percentile of the normalized discharge for the corresponding rainfall event is calculated as:

$$HI_{Q_j} = C_{RL\_Q_j} - C_{FL\_Q_j} \quad (3)$$

where HI_{Q_j} is the hysteresis index at percentile j of the normalized discharge; and $C_{RL\_Q_j}$ and $C_{FL\_Q_j}$ are the normalized concentrations at percentile j of the normalized discharge on the rising and falling limbs, respectively. If there is no measured concentration value at the equivalent discharge point on the rising or falling limb, linear interpolation is used to generate a value on the corresponding limb ($C_{RL\_Q_j}$ or $C_{FL\_Q_j}$, respectively). Then, the final HI for the rainfall event is the mean of all hysteresis indexes at a specific percentile of the normalized discharge. In this study, the hysteresis index at every 10% of the discharge was calculated (Lloyd et al., 2016). The water age is treated as a proxy for a specific tracer "concentration", and the hysteresis index of the water age for each rainfall event was calculated with Eq. (1) to (3). The value of the hysteresis index varies between −1 and 1. Negative and positive values indicate anti-clockwise and clockwise loops, respectively. The absolute value of the hysteresis index indicates the size of the hysteresis loop representing the degree of lag between the responses of the discharge and concentration or water age.

3. Results

3.1. Temporal dynamics of NO_3-N concentration, loading and age of underground conduit flow

Fig. 2 shows the time series of the precipitation, discharge, NO_3-N concentration, loading and flow age during the study period encompassing one full dry season (November 2016 to April 2017) and one full wet reason (May to October 2017). The total precipitation was 1,017 mm, with a maximum hourly rainfall of 45.6 mm. The mean discharge, NO_3-N concentration and NO_3-N loading were 5×10^{-3} m^3/s, 3.72 mg/L and 0.067 kg/h, respectively. Notable variations in underground conduit flow between the dry and wet seasons were evident from the flow duration curves from hourly observations. The highly developed drainage systems in karstic hydrogeology causes a sharp rise and decline of the hydrograph during the wet season. For example, the discharge can vary by three orders of magnitude within a short time (Fig. 2b). The variability of NO_3-N concentration was much lower than that of the flow over the study period, although there were several peaks both in the dry and wet seasons (Fig. 2c). In general, NO_3-N concentrations were in a low level with the mean value of 3.4 mg/L during dry season, and that were in a relatively high level with the mean value of 4 mg/L during wet season. It was notable that, immediately after fertilization (October-November and May-June), the increases of NO_3-N concentrations of underground conduit flow were marked when there was rainfall (Fig. 2c), and then the NO_3-N concentrations declined gradually with time. The variability of the NO_3-N loading was, as expected, similar to that of flow, exhibiting a marked seasonality (Fig. 2d). In particular, nitrate export in underground conduit drainage was directly related to heavy rainfall conditions, showing sharp increases after heavy storms. Affected by mixing of pre-event and event water (younger water), the age of underground conduit flow derived from the tracer-aided model revealed a clear seasonality, with a mean value of 531 and 271 days the dry and wet season, respectively (Fig. 2e). Notably, the flow age exhibited dramatic changes after heavy rainfall (decreasing from ~ 500 days to 1 day), especially during the transition period between the dry and wet seasons (Fig. 2e). Summary statistics of the precipitation, discharge, NO_3-N concentration, loading and flow age during the study period are shown in Table 1.

3.2. Relationships between nitrate concentration/loading and discharge/age of underground conduit

Fig. 3 shows the relationships between the measured discharge, NO_3-N concentrations and loadings during the study period. The C-Q pattern is classified using a simple power law $C = aQ^b$ with exponent b indicating the C-Q archetype, which reflects the integration of hydrological processes and biogeochemical reactions at the catchment scale (Godsey et al., 2009; Musolff et al., 2015). Exponent b is 0.03 in the fitting of the hourly NO_3-N concentration and discharge in underground conduit at the catchment outlet. This reveals a generally constant pattern (absolute $b < 0.1$ (Thompson et al., 2011)), indicating relatively small variations in NO_3-N concentrations compared to discharge. However, there are many banded or "noisy" variations in NO_3-N concentration with the discharge associated with specific rainfall events (Fig. 3). Which suggests that different C-Q patterns may appear under different hydroclimatic situations, contrasting antecedent and fertilization conditions. In contrast, the hourly NO_3-N loading in underground conduit flow increases almost linearly with the discharge.

The wide ranges of flow age at catchment outlet could provide further insight into the temporal dynamics of flow paths and mixing

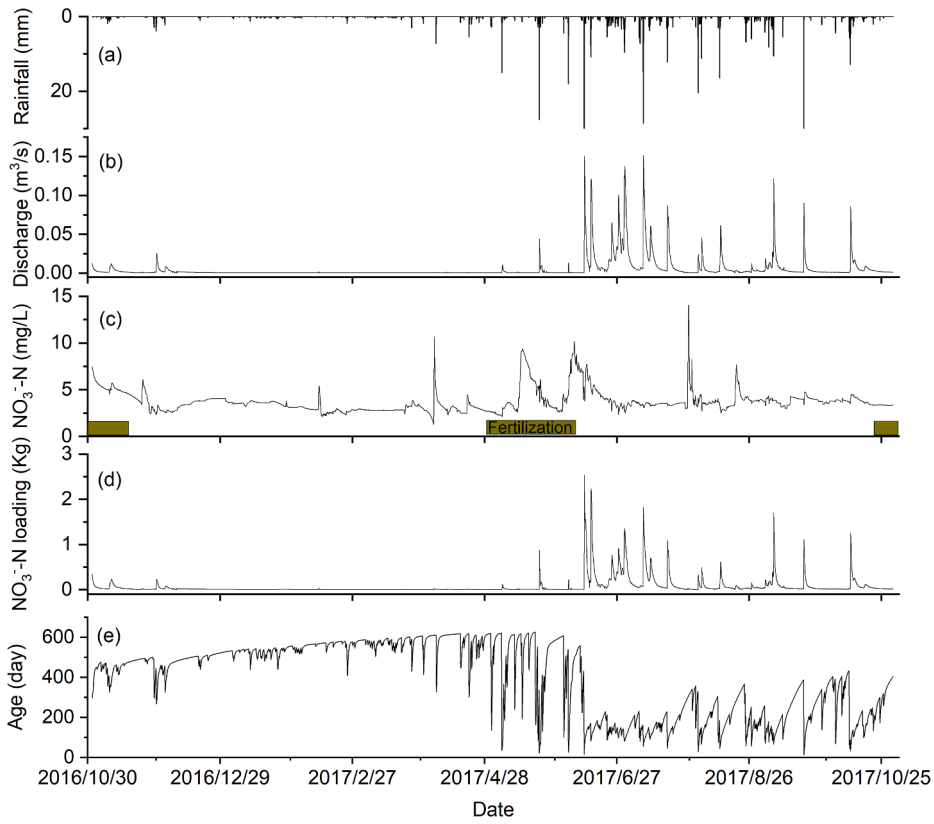

Fig. 2. Time series of hourly (a) precipitation, (b) discharge, (c) in situ NO_3-N concentration, (d) NO_3-N loading, and (e) water age. The shading in (c) shows the time schedule of fertilization.

Table 1
Summary statistics of the hourly variables measured in the Chenqi catchment during the study period.

Data	Unit	Minimum	Maximum	Mean	Coefficient of variation (CV)
Rainfall	mm	0	45.6	0.1	8.8
Discharge	m^3/s	0.0002	0.151	0.005	2.9
[NO_3-N]	mg/L	1.3	14.1	3.7	0.3
NO_3-N loading	kg	0.001	2.54	0.07	2.8
Age	day	1	627	400	0.44

processes affecting the spatial–temporal variations in nitrate fate at the catchment scale. The changes in NO_3-N concentration and loading with the flow age derived from the tracer-aided model are shown in Fig. 4. The results showed that the correlation between hourly NO_3-N concentrations and flow age in the underground conduit was not significant. This is consistent with the findings that nitrate concentration dynamic in conduit flow in karst catchment are affected by multiple factors, such as N sources, rainfall amount and intensity, flow paths, biogeochemical interactions and mixing processes (Yue et al., 2020; Zhang et al., 2020a; 2020b;; Husic et al., 2019). In contrast, there was a significant negative correlation between the monthly NO_3-N concentration and flow age during dry season ($R^2 = 0.8$, with the significance level of 0.05). That was probably due to the more limited variation in hydrological conditions causing biogeochemical reactions (e.g. denitrification) to be the main controlling factor for NO_3-N concentrations in underground conduit flow. Due to the changeable hydrometeorological conditions and biogeochemical processes, there was a weak positive correlation between the monthly NO_3-N concentration and flow age during wet season ($R^2 = 0.11$, significance level 0.05).

The monthly NO_3-N loadings showed a dominant decrease with increasing of flow age during both dry and wet seasons, and the negative correlation was more pronounced for the dry season ($R^2 = 0.81$) than that for the wet season ($R^2 = 0.24$). While the mean NO_3-N loadings during the wet season (0.12 kg/h) were much higher than that during the dry season (0.01 kg/h). Obviously, the high NO_3-N loadings corresponded to some specific flow age ranges during both dry and wet seasons. For example, during the dry season, highest NO_3-N loadings mainly occurred when the flow ages varied between ~ 250 and 450 days. During the wet season, the high NO_3-N loadings corresponded to flow ages<200 days, e.g., the maximum NO_3-N loading was 2.5 kg/h when the water age was 61 days (Fig. 4a). In general, the NO_3-N loadings changed sharply (from ~ 0.1 to 2.6 kg/h) when the flow age ranges were between ~ 30 to 150 days during the wet season.

3.3. Nitrate concentration and flow age hysteresis behaviours in rainfall events

To examine the hysteresis of nitrate concentration and flow age with respect to discharge and its control of flow paths and mixing, a total of 15 rainfall events during the study period were selected for analysis, with 3 events in dry season and 12 events in wet season (Table 2). A rainfall event here is defined as a rain period in which there is no continuous 24 h spell without rainfall. Of these 15 selected rainfall events, the maximum rain amount was 86.8 mm and the minimum rain amount was 7.7 mm. The mean discharges were 0.005 and 0.037 m^3/s for the 3 rainfall events in dry season events and the 12 rainfall events in wet season events, respectively. The mean age of the underground conduit flow in the dry season rainfall events (416 days) was approximately 3.4 times that in the wet season events (121 days). While the difference of NO_3-N concentration between dry and wet season rainfall events was relatively small, with mean values of 3.5 and 3.9 mg/L, respectively. The correlations between hourly discharge and NO_3-N

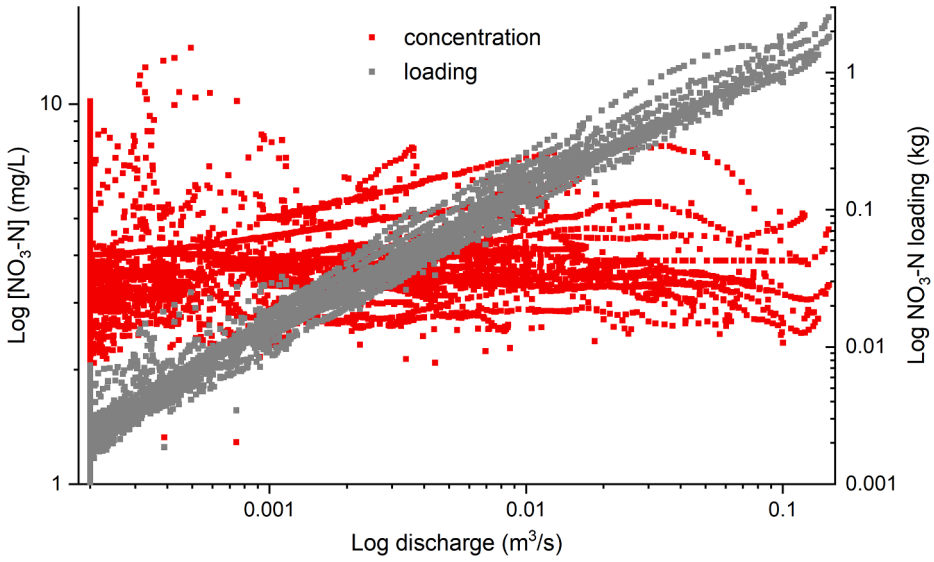

Fig. 3. Hourly NO_3-N concentration and loading vs. discharge over the study period.

concentration, flow age in underground conduit for the 15 chosen rainfall events were estimated in this study (Fig. S1 in Appendix). Although some of them were not significant due to multiple confounding influences, it could provide potential indications for flow paths and mixing processes. The results showed that the flow age and discharge (A-Q) were negatively correlated for all 15 rainfall events (Table 2), which indicated that the rain water caused the decline of modelled age of underground conduit flow. In contrast, the relationships between NO_3-N concentration and discharge (C-Q) were more complex. A negative correlation between NO_3-N concentration and discharge occurs in 9 of the 12 rainfall events in wet season, while the other 3 wet season rainfall events, as well as the 3 rainfall events during dry season exhibited a positive correlation (Table 2). It is worth noting that the 6 rainfall events with positive correlation between NO_3-N concentration and discharge occurred immediately after or close to fertilization (May-June and October-November), and the other rainfall events with negative correlation were in mid and later wet season. This reveals that N supply conditions have a significant influence on nitrate dynamics of underground conduit flow in rainfall event.

Fig. 5 shows the inter-relationships of discharge, NO_3-N concentration and flow age for two representative rainfall events in the dry and wet seasons, respectively. Those for the remaining selected rainfall events are in Fig. S2 in the Appendix. The results showed that the A-Q relationship for each of all the 15 selected rainfall events exhibited an anti-clockwise loop pattern, implying that the mean flow age on the rising limb of the hydrograph was lower than that on the falling limb. Which revealed that the response of flow age to rainfall was quicker than that for discharge. The absolute values of A-Q hysteresis index of rainfall events in dry season (mean = 0.64 for Events 1,2 and 3) were significantly higher than that in the wet season (mean = 0.24 for Events 4 to15), which indicated that in general, the time lag between age and discharge was smaller for the wet season than for the dry season. For example, the mean time lag between the lowest age and discharge peak was 10 h for rainfall events in the dry season, and that was 4 h for rainfall events in wet seasons.

For NO_3-N concentrations, the three rainfall events in dry season exhibited anti-clockwise hysteresis with negative hysteresis index values, indicating that the mean NO_3-N concentration of underground conduit flow was lower on rising limb of hydrograph than that on falling limb. Which revealed that the NO_3-N concentration peak occurred later than discharge peak. In these three rainfall events, the NO_3-N concentrations of underground channel flow eventually exceeded the corresponding initial level. This could be due to the mobilization of external nitrate in soil (e.g. fertilizer) by rainfall. This is consistent with the positive correlation between NO_3-N concentrations and discharge (govern by rainfall) in Table 2. Eight of the 12 rainfall events in wet season exhibited a "figure-of-eight" or complex loop pattern, which indicates the complexity of NO_3-N concentration dynamics and its hysteresis behaviour in the wet season. Although not all rainfall events showed simple unidirectional loops, the method of hysteresis index in this study effectively normalises the hydrograph and examines the relative behaviour of the rising and falling limb, thereby identifying the proportion of the rainfall event occurring in a clockwise or anti-clockwise phase (Lloyd et al., 2016). Therefore, the hysteresis indexes for all rainfall events were calculated for assessment of their inter-relationships between NO_3-N concentration and discharge (Table 2). The results showed that 7 of the 12 rainfall events in wet season had positive hysteresis index indicating higher mean NO_3-N concentration on the rising limb of hydrograph than that on the falling limbs, which reveals abundant nitrate supply during the rising limb period. In contrast, the negative hysteresis index values for the other 5 rainfall events in wet season suggest the limited supply of nitrate to underground conduit at the beginning of rainfall event.

It is worth noting that there was a notable decline of NO_3-N concentration at the start of each rainfall event in both dry and wet seasons (Fig. 5 and S2), which implied that a part of rain water with low NO_3-N concentration entered the underground conduit quickly just after rainfall started. This decline in NO_3-N concentration was almost synchronous with age decline of underground conduit flow in dry season, which implies that the event water with low age draining through preferential flow paths leads to the attenuation of nitrate in underground conduit flow. However, the time lags between the lowest flow age and peak NO_3-N concentrations of conduit flows were significantly longer for rainfall events in wet season than that in dry season. For example, the mean time lag between lowest flow age and peak NO_3-N concentration was close to 0 for the three dry season rainfall events, but increased to ~ 5 h for the 12 rainfall events in wet season. This is most likely caused by the greater transport capacity for mobilizing nitrate by heavy rainfall in the wet season, which delays the decline in NO_3-N concentration of underground conduit flow. This is consistent with the findings in other studies that more nitrate is produced as soils become wetter, and successive rainfall events can facilitate greater nitrate leaching as catchments become more hydrologically connected (Rusjan et al., 2008; Hansen and Singh 2018).

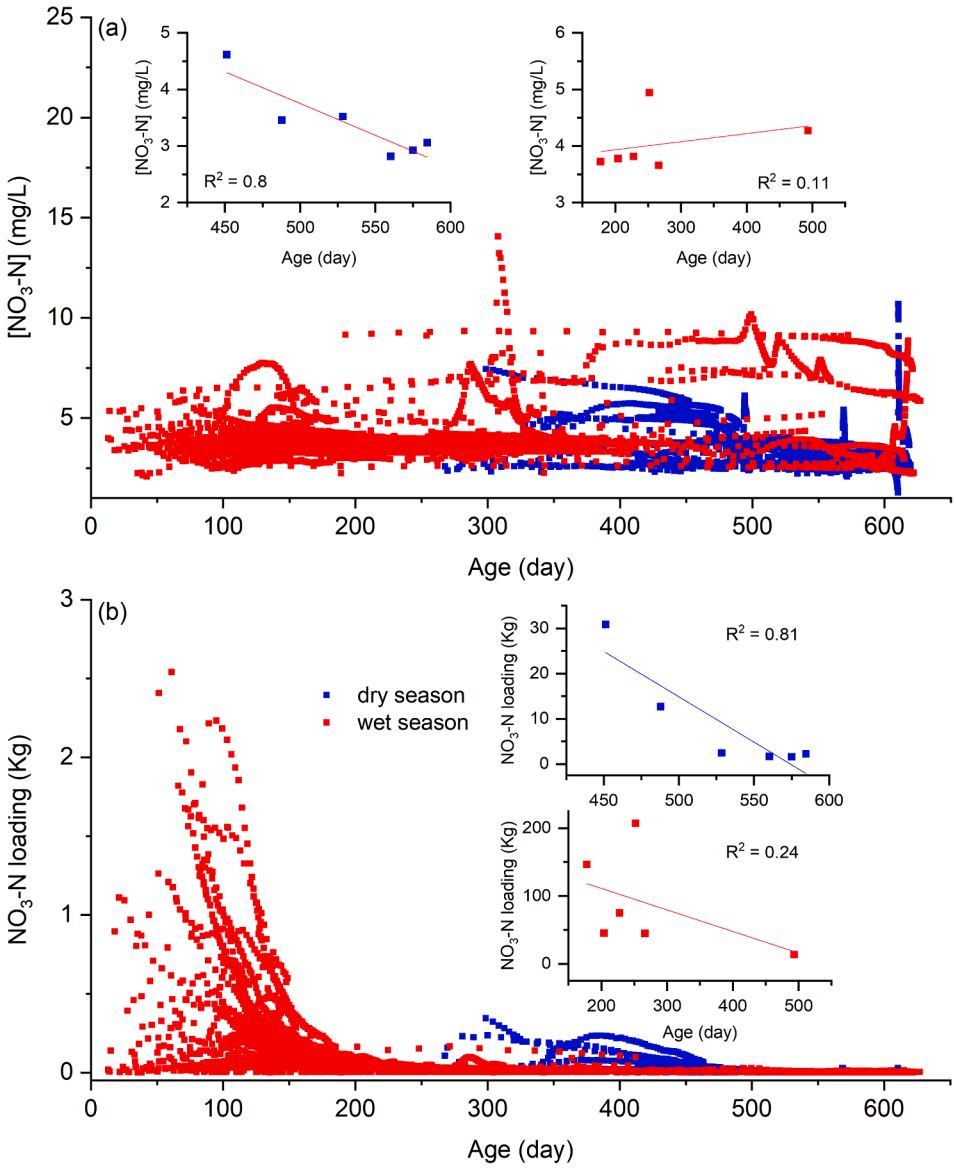

Fig. 4. NO_3-N concentration (a) and NO_3-N loading (b) versus water flux age at the catchment outlet using the hourly data series (the inset plots are based on monthly values).

Table 2
Statistics of the rainfall, discharge, NO_3-N concentration, water age, C-Q hysteresis index and A-Q hysteresis index for the 15 rainfall events.

Event	Rainfall (mm)	Discharge (m^3/s) × 10^{-3}		[NO_3-N] (mg/L)		Age (day)		C-Q Index	A-Q Index
		mean	Range	mean	range	mean	range		
2016/11/8	18.9	4.8	1.1–12	5.1	4.5–5.7	424	326–463	−0.46↗	−0.61↘
2016/11/29	25.4	5.6	0.8–25.7	2.8	2.3–3.4	400	268–462	−0.48↗	−0.62↘
2016/12/3	7.7	5.3	1.7–8.5	2.7	2.5–2.8	423	325–466	−0.5↗	−0.68↘
2017/6/4	26.8	4.7	0.2–13.2	5.2	4.4–6.5	76	27–212	−0.74↗	−0.52↘
2017/6/12	86.8	42.9	0.3–150.8	6.1	3.8–7.8	123	4–207	−0.16↗	−0.16↘
2017/6/15	29	37.9	7.6–121.7	5.1	4.4–5.7	143	10–185	0.27↘	−0.47↘
2017/6/24	27.8	35.1	15.2–64.9	3.6	2.7–3.9	145	16–172	−0.37↘	−0.28↘
2017/6/27	26	59.2	30.6–100.1	3	2.4–3.5	126	14–150	0.05↘	−0.3↘
2017/6/30	51.6	76.4	28.7–137.4	3.1	2.5–3.7	108	8–134	0.13↘	−0.02↘
2017/7/8	81.4	82.5	5.7–151.3	3.3	3.1–3.5	95	6–163	0.24↘	−0.2↘
2017/7/12	16.2	31.9	14.9–61.1	3.3	3.2–3.5	126	20–161	0.01↘	−0.11↘
2017/8/2	26.6	7.9	0.2–24.1	4	3.3–4.5	107	10–150	−0.11↘	−0.19↘
2017/8/4	13.6	16.1	2.9–45.4	3.5	2.7–4.2	128	26–162	0.2↘	−0.17↘
2017/8/12	29	14.1	1.9–61.9	2.9	2.5–3.6	149	13–217	0.28↘	−0.13↘
2017/10/10	45	32.6	2.7–85.8	4.3	3.5–4.5	97	9–138	−0.78↗	−0.29↘

C: [NO_3-N]; Q: discharge; A: water age. ↗ indicates a positive correlation, and ↘ indicates a negative correlation between NO_3-N concentration/water age and discharge. All correlations are at the significance level of 0.05.

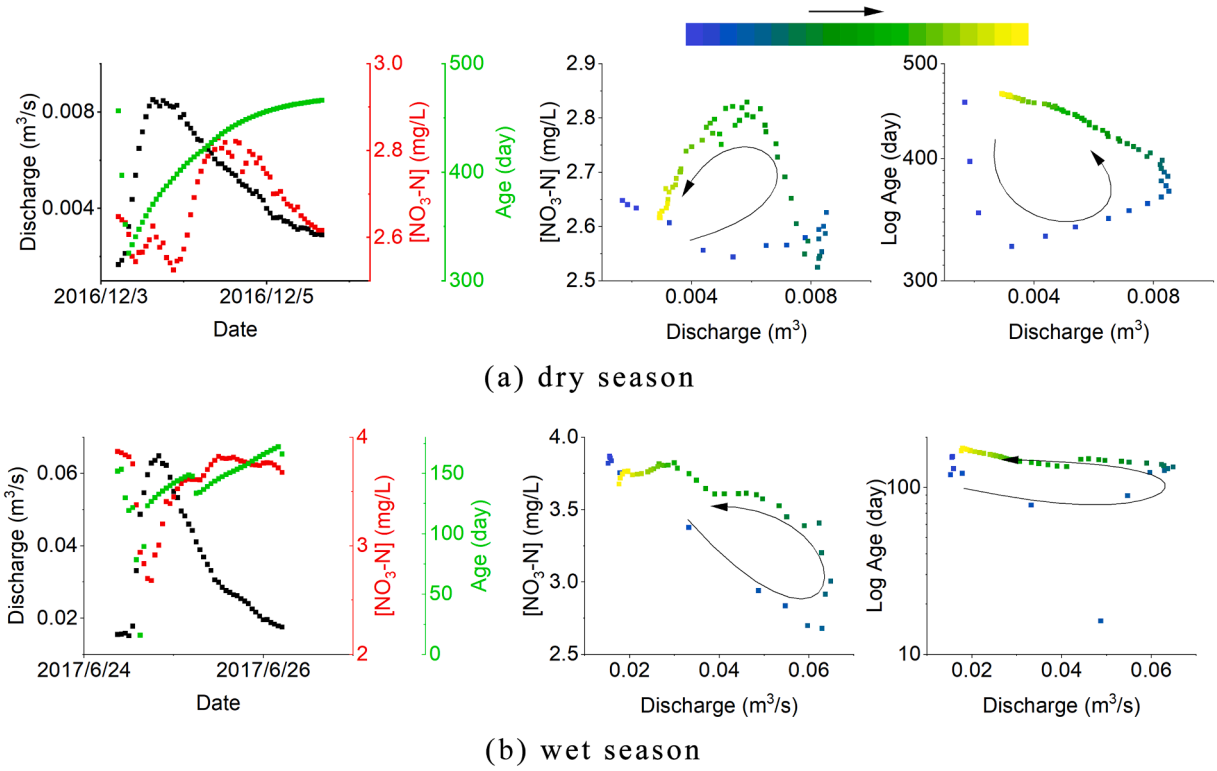

Fig. 5. The inter-relationships between discharge, NO_3-Nconcentration and flux age (1st column), NO_3-N concentration vs. discharge (2nd column) and age vs. discharge (3rd column) for one of the 15 rainfall events during the dry season (a) and wet season (b). The plots for all rainfall events (15) are provided in the Appendix.

3.4. NO_3-N export with catchment drainage driven by specific rainfall events

To assess how NO_3-N export in underground conduit flow was driven by specific rainfall events, three events (Event 2, 7 and 12 out of the 15 events listed in Table 2) with similar rainfall amounts (~26 mm) were selected for the analysis. The three events on t1, 28 November 2016 (dry season), t2, 26 June 2017, and 2 August 2017 (wet season). The NO_3-N export with the underground conduit flow driven by each rainfall event was estimated using the flux tracking method described in the Methodology section.

The intensity and duration of rainfall for the three selected events were notably different, e.g., there were 35, 40 and 5 rain hours in the three events with similar rainfall amounts. The maximum hourly rainfall intensity for each event was 3.9, 2.8 and 20.4 mm, respectively (Fig. 6f). As expected, the amount of NO_3-N export driven by the rainfall events in dry season was notably lower than in the wet season (Fig. 6c, d and e). For Event 2 in the dry season, approximately 9.25 kg NO_3-N was exported with the underground conduit flow over the period from the entry time of rainwater to the end of the study period (a total of 336 days). In contrast, the same NO_3-N export amount driven by the 7th and 12th events in the wet season only required 4 and 2 days, respectively. The highest NO_3-N export rate for Event 2 (in dry season) was 0.57 kg/d occurring 223 days after the rainfall (Fig. 6c), which implies that most of the entering rainwater was stored in the critical zone during dry periods and released during wet periods resulting in relatively high NO_3-N transport under high wetness condition. The maximum NO_3-N export rates of Events 7 and 12 were 5.9 and 9.1 kg/d, respectively (Fig. 6d and e), which both occurred at the beginning of the rainfall events (the 4th and second days, respectively, after the initial rainfall). It seems that the higher NO_3-N export rate of Event 12 is due to the high rainfall intensity. From the results, although the rainfall occurring in dry season is unable to connect to drainage networks and transport large amounts of nitrate out of catchment in a short time, the nitrate export in wet season driven by the 'old' water from previous rainfall should not be ignored.

4. Discussion

The dynamics of solute concentrations and loading, and their relationships to water age in streamflow are mainly controlled by both supply and transport conditions, which have been widely reported for non-karst catchments (Reddy et al., 2011; Tunaley et al., 2016; van Metre et al., 2016). Compared to most non-karst catchments, the variations in flow paths and mixing processes under different hydrometeorological and critical zone structure conditions in a karst landscapes are more dramatic (Hartmann et al., 2014). Especially, partial mixing usually occurs in the karst critical zone with notable shifts between fast flow (e.g., the flow within macropores) and slow flow (e.g., matrix flow) (Van Schaik et al., 2008; Legout et al., 2009). This implies that during the same rainfall event, poorly mixed water in proximal zones to drainage networs and the well-mixed water in more distal areas impose both dilution and enrichment effects on underground conduit flow, respectively. This inference is consistent with the findings that connectivity between the solute source and stream causes the variations in solute concentration and C-Q pattern of the streamflow (Herndon et al., 2015; Schwab et al., 2017). From these inferences and the results of this study, a conceptual model of flow and N transport in the karst catchment can be developed (Fig. 7).

Due to intense fertilization on farm land, surface soil in the depression is the largest nitrogen reservoir in the catchment. Hence, the nitrate supply of underground conduit flow is mainly controlled by the infiltrated flow in that can mobilize N from the surface soil layer and transport it. During the dry season, the high contribution of water from small fractures in the slow flow reservoir results in high ages of underground conduit flow (Fig. 7a). Since the small fracture water has less contact with the surface soil, it transports less nitrate to underground

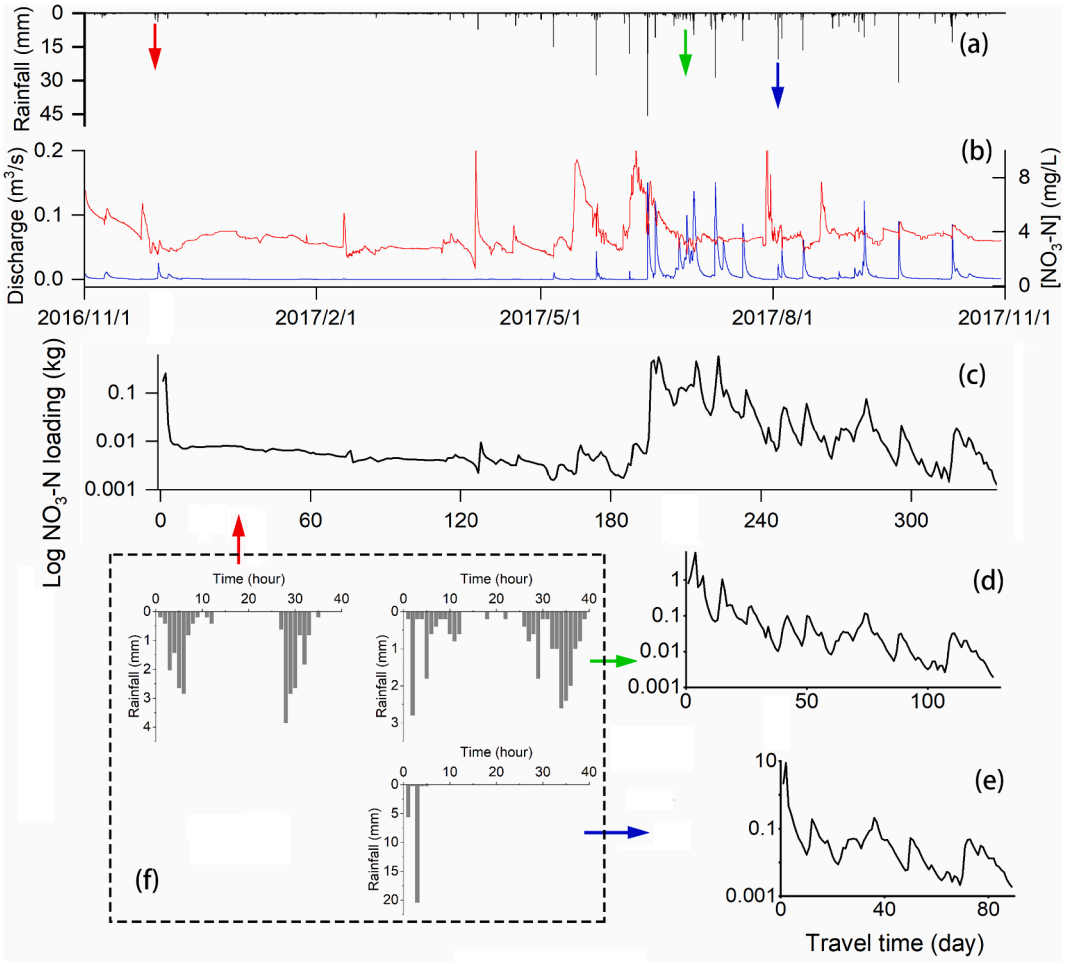

Fig. 6. Temporal dynamics of NO_3-N export with the underground flow caused by rainwater entry at the different reference times. (a) and (b) show the rainfall, discharge (red) and NO_3-N concentration (red). (c), (d) and (e) show the temporal dynamics of NO_3-N export caused by rain events 1, 2 and 3, respectively, and (f) shows the hourly rainfall distribution of the three rain events.

conduit. Even if there is some infiltrated water from deeper soil layers draining to fractures or conduits, this will bring in less nitrate due to denitrification. It can be inferred that small fractures provide an anaerobic environment due to their tiny spaces under soil and rock cover, which enhances the denitrification leading higher nitrate removal (Tesoriero and Puckett, 2011; Heffernan et al., 2012; Kolbe et al., 2016; Benettin et al., 2020). Although the small fractures have not received much attention, they may be another important underground "hot spot" for denitrification leading to nitrate removal in karst catchments. Therefore, underground conduit flow usually exhibits a gradual decline or relatively constant pattern in nitrate concentration during dry season, especially during no rain period (Fig. 2). This is also consistent with the negative correlation between NO_3-N concentration and flow age during dry season (Fig. 4). When rainfall occurs in the dry season, part of the rainfall rapidly infiltrates through large fractures at beginning of the event leading a decline in the age of the underground conduit flow (Fig. 7b). Due to the high percolation rate, this quick infiltrated water has less contact time with surface soil, meaning little leaching of nitrate and poor mixing with pre-event soil water, which also leads a drop in NO_3-N concentrations of conduit flow. Hence, although large fractures account for a small proportion in karst aquifer (approximately 8% by Zhang et al., 2013), they can impose dominant effects on water and solute transport processes in karst critical zone. Consequently, the well-mixed water with more leached nitrate enters underground conduit resulting in a significant increase in NO_3-N concentration of conduit flow (Fig. 7b).

Generally, the low ages of the underground conduit flow during wet season depends on the high contributions of event water from rapid flow through large fractures or sinkholes (Fig. 7c). However, the NO_3-N concentrations of underground conduit flow vary greatly in different stages of the wet season due to the influence of nitrate supply conditions. The heavy fertilization that occurs at beginning of wet season (May-June) leads abundant storage of nitrate in soil layer during this period. With the increase of hydrological connectivity between surface and underground conduits, greater infiltration of soil water with high NO_3-N concentration cause a relatively high level of NO_3-N concentrations in underground conduit flow, especially during the period immediately after fertilization. As NO_3-N transport and removal (e.g. denitrification and plant uptake) progresses, the NO_3-N storage in the soil layer gradually decreases. In addition, the increase of rainfall enhances solute dilution during the middle and later wet season (e.g. July and August), which leads a relatively low level in NO_3-N concentrations of underground conduit flow. From these variations, it can be inferred that the main controlling condition changes from transport limited at the beginning of wet season to supply limited at the middle and latter of wet season. The pattern of decline then increase in nitrate concentration of underground conduit flow for rainfall event in the wet season is similar to that in dry season (Fig. 7d). And the high contribution of hillslope flow enhances the dilution of the underground conduit flow under high wetness condition. Unlike in the dry season, the NO_3-N concentrations of underground conduit flow usually return to the pre-event levels after the rainfall event due to the supply limited condition.

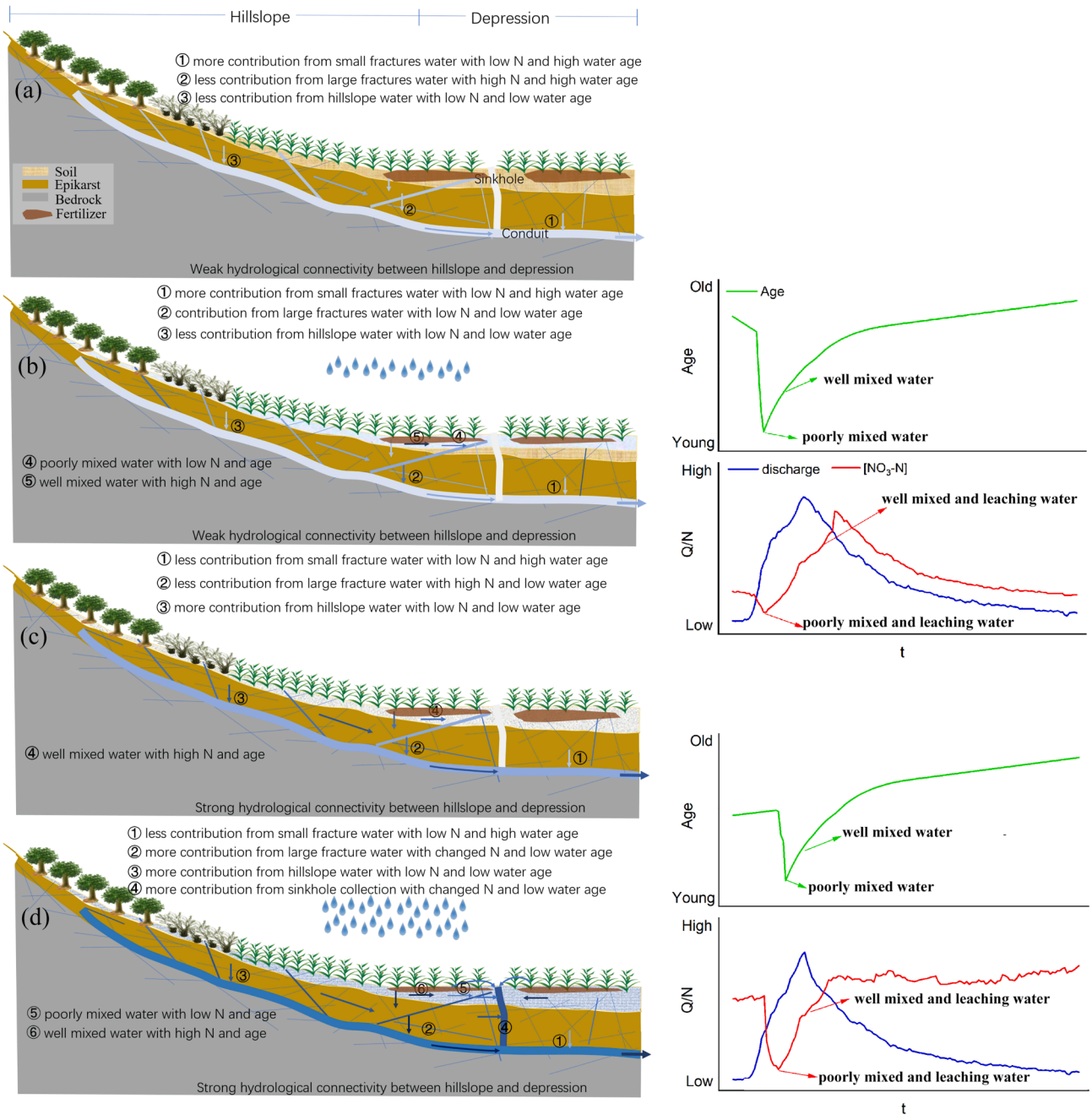

Fig. 7. Conceptual diagram illustrating the flow processes under the different hydroclimatic conditions and their controlling effect on the water age and NO_3-N dynamics in the karst critical zone. (a) no rain period in dry season; (b) rain period in dry season; (c) no rain period in wet season; (d) rain period in wet season.

Wider implication from this study is the controlling influence of the soil-rock interface on nitrate transport in karst catchment. The time lags of NO_3-N concentration peak to discharge peak for some rainfall events are only several hours (Fig. S2), even in the dry season. From previous studies in this catchment, the soil thickness is ~ 2 m, and the hydrological conductivity of the soil is about 10^{-5} m/s for the lower cultivated areas (Zhang et al., 2011). According to this, from first approximations, it will take more than ~ 56 h for rain water and NO_3-N to enter into underground conduit through soil matrix. Hence, there may be preferential paths connecting the soil to the underground conduit for water and NO_3-N infiltration. Wang et al. (2020) reported that high proportion of nitrate loss from peak clusters and lowland farmland during heavy rainfall events based on nitrate isotopes, which supports this explanation. In the south-western karst area of China, soil layer in depression for agriculture is usually interspersed with rocks. Therefore, the soil-rock interface may provide the fast pathways for high nitrate fluxes, especially in the wet season after fertilization.

5. Conclusion

In this study, water age was linked to nitrate dynamics in underground conduit flow from a 1.25 km^2 karst catchment in southwestern China. A tracer-aided model for the catchment developed by Zhang et al. (2019) and calibrated on flows and stable isotopes, was adopted to determine the age of underground conduit flow. High-frequency measurements allowed us to examine the inter-relationships between nitrate and discharge dynamics and their connections with the flow age. The variations in flow age and nitrate concentration/loading are mainly controlled by flow pathways and mixing processes in karst catchment. High contribution of small fracture water leads a low nitrate

concentration and a negative correlation between nitrate concentrations and flow age in underground conduit flow during dry season. Which implies that the small fractures may be another important "hot spot" for denitrification causing nitrate removal in the karst critical zone. The changes between transport limited and supply limited conditions cause the marked variations in nitrate concentration of underground conduit flow. The notable dilution effects of event water via fast flow path cause a sharp drop in age and nitrate concentration of the underground conduit flow at the beginning of rainfall. While the mobilization of nitrate in surface soil layers leads the increase of nitrate concentration at the middle and latter of rainfall. The ability to transport nitrate out of the catchment can be potentially enhanced when 'old' water is displaced and mobilized under high wetness conditions.

This study reports advances in integrating of tracer-aided model and higher-frequency observation of nitrate in linking nitrate dynamics to water age, which provides crucial insight into nitrate transport and mixing in complex karst environments. This highlights the karstic landform and critical zone features controlling on variations in nitrate transport in karst catchments which will improve our ability to evaluate the effects of climate change and agricultural management on nitrate pollution help underpin decision support tools. However, the controls on nitrate dynamics and associated water age in the different landscape units in karst catchments requires further research, which will necessitates longer and more detailed spatio-temporal observation data, e.g., nitrate concentration in the hillslopes, wells and fractures in the epikarst.

CRediT authorship contribution statement

Zhicai Zhang: Conceptualization, Methodology, Software, Writing - original draft. **Xi Chen:** Conceptualization, Writing - review & editing, Supervision. **Siliang Li:** Validation, Conceptualization. **Fujun Yue:** Data curation, Resources. **Qinbo Cheng:** Investigation, Data curation. **Tao Peng:** Data curation, Resources. **Chris Soulsby:** Writing - review & editing, Supervision.

Declaration of Competing Interest

The authors declare that they have no known competing financial interests or personal relationships that could have appeared to influence the work reported in this paper.

Acknowledgments

This research was supported by the National Key Research and development Program of China (2016YFC0502602), the National Natural Science Foundation of China (41971028), and the UK Natural Environment Research Council MIDST-CZ Project (NE/S009167/1). We thank the two anonymous reviewers and the editor for their constructive comments which significantly improved the manuscript.

Appendix A. Supplementary data

Supplementary data to this article can be found online at https://doi.org/10.1016/j.jhydrol.2020.125699.

References

Barnes, R.T., Raymond, P.A., 2009. The contribution of agricultural and urban activities to inorganic carbon fluxes within temperate watersheds. Chem. Geol. 266, 318–327.
Basu, N.B., Destouni, G., Jawitz, J.W., Thompson, S.E., Loukinova, N.V., Darracq, A., Zanardo, S., Yaeger, M., Sivapalan, M., Rinaldo, A., Rao, P.S.C., 2010. Nutrient loads exported from managed catchments reveal emergent biogeochemical stationarity. Geophys. Res. Lett. 37 https://doi.org/10.1029/2010GL045168.
Benettin, P., Bailey, S.W., Campbell, J.L., Green, M.B., Rinaldo, A., Likens, G.E., McGuire, K.J., Botter, G., 2015. Linking water age and solute dynamics in streamflow at the Hubbard Brook Experimental Forest, NH, USA. Water Resour. Res. 51, 9256–9272.
Benettin, P., Fovet, O., Li, L., 2020. Nitrate removal and young stream water fractions at the catchment scale. Hydrol. Process. 34, 2725–2738.
Bieroza, M.Z., Heathwaite, A.L., 2015. Seasonal variation in phosphorus concentration–discharge hysteresis inferred from high-frequency in situ monitoring. J. Hydrol. 524, 333–347.
Birkel, C., Soulsby, C., 2015. Advancing tracer-aided rainfall-runoff modelling: a review of progress, problems and unrealised potential. Hydrol. Process. 29, 5227–5240.
Botter, G., 2012. Catchment mixing processes and travel time distributions. Water Resour. Res. 48 https://doi.org/10.1029/2011WR011160.
Botter, G., Bertuzzo, E., Rinaldo, A., 2011. Catchment residence and travel time distributions: The master equation. Geophys. Res. Lett. https://doi.org/10.1029/2011GL047666.
Bowes, M.J., Jarvie, H.P., Halliday, S.J., Skeffington, R.A., Wade, A.J., Loewenthal, M., Gozzard, E., Newman, J.R., Palmer-Felgate, E.J., 2015. Characterising phosphorus and nitrate inputs to a rural river using high-frequency concentration–flow relationships. Sci. Total Environ. 511, 608–620.
Chen, X., Zhang, Z., Soulsby, C., Cheng, Q., Binley, A., Jiang, R., Tao, M., 2018. Characterizing the heterogeneity of karst critical zone and its hydrological function: An integrated approach. Hydrol. Process. 32, 2932–2946.
Di, H.J., Cameron, K.C., 2002. Nitrate leaching in temperate agroecosystems: Sources, factors and mitigating strategies. Nutr. Cycl. Agroecosystems. 64 (3), 237–256.
Duncan, J.M., Band, L.E., Groffman, P.M., 2017. Variable nitrate concentration-discharge relationships in a forested watershed. Hydrol. Process. 31, 1817–1824.
Fenton, O., Mellander, P.-E., Daly, K., Wall, D.P., Jahangir, M.M.R., Jordan, P., Hennessey, D., Huebsch, M., Blum, P., Vero, S., Richards, K.G., 2017. Integrated assessment of agricultural nutrient pressures and legacies in karst landscapes. Agric. Ecosyst. Environ. 239, 246–256.
Ford, D., Williams, P., 2007. Karst Hydrogeology and Geomorphology. Karst Hydrogeology and Geomorphology. John Wiley & Sons Ltd, West Sussex, England.
Godsey, S.E., Kirchner, J.W., Clow, D.W., 2009. Concentration-discharge relationships reflect chemostatic characteristics of US catchments. Hydrol. Process. 23, 1844–1864.
Hartmann, A., Goldscheider, N., Wagener, T., Lange, J., Weiler, M., 2014. Karst water resources in a changing world: Review of hydrological modeling approaches. Rev. Geophys. 52, 218–242.
Heaton, T.H.E., Stuart, M.E., Sapiano, M., Micallef Sultana, M., 2012. An isotope study of the sources of nitrate in Malta's groundwater. J. Hydrol. 414–415, 244–254.
Heffernan, J.B., Albertin, A.R., Fork, M.L., Katz, B.G., Cohen, M.J., 2012. Denitrification and inference of nitrogen sources in the karstic Floridan Aquifer. Biogeosciences 9, 1671–1690.
Heidbüchel, I., Troch, P.A., Lyon, S.W., 2013. Separating physical and meteorological controls of variable transit times in zero-order catchments. Water Resour. Res. 49, 7644–7657.
Herndon, E.M., Dere, A.L., Sullivan, P.L., Norris, D., Reynolds, B., Brantley, S.L., 2015. Landscape heterogeneity drives contrasting concentration–discharge relationships in shale headwater catchments. Hydrol. Earth Syst. Sci. 19, 3333–3347.
Hrachowitz, M., Soulsby, C., Tetzlaff, D., Dawson, J.J.C., Malcolm, I.A., 2009. Regionalization of transit time estimates in montane catchments by integrating landscape controls. Water Resour. Res. 45 https://doi.org/10.1029/2008WR007496.
Husic, A., Fox, J., Adams, E., Ford, W., Agouridis, C., Currens, J., Backus, J., 2019. Nitrate Pathways, Processes, and Timing in an Agricultural Karst System: Development and Application of a Numerical Model. Water Resour. Res. 55, 2079–2103.
Kellman, L.M., Hillaire-Marcel, C., 2003. Evaluation of nitrogen isotopes as indicators of nitrate contamination sources in an agricultural watershed. Agric. Ecosyst. Environ. 95, 87–102.
Kirchner, J.W., 2016a. Aggregation in environmental systems – Part 1: Seasonal tracer cycles quantify young water fractions, but not mean transit times, in spatially heterogeneous catchments. Hydrol. Earth Syst. Sci. 20, 279–297.
Kirchner, J.W., 2016b. Aggregation in environmental systems – Part 2: Catchment mean transit times and young water fractions under hydrologic nonstationarity. Hydrol. Earth Syst. Sci. 20, 299–328.
Kirchner, J.W., Feng, X., Neal, C., 2000. Fractal stream chemistry and its implications for contaminant transport in catchments. Nature 403, 524–527.
Legout, A., Legout, C., Nys, C., Dambrine, E., 2009. Preferential flow and slow convective chloride transport through the soil of a forested landscape (Fougères, France). Geoderma 151, 179–190.
Liu, C.-Q., Li, S.-L., Lang, Y.-C., Xiao, H.-Y., 2006. Using δ 15 N- and δ 18 O-Values To Identify Nitrate Sources in Karst Ground Water, Guiyang, Southwest China. Environ. Sci. Technol. 40, 6928–6933.
Lloyd, C.E.M., Freer, J.E., Johnes, P.J., Collins, A.L., 2016. Using hysteresis analysis of high-resolution water quality monitoring data, including uncertainty, to infer controls on nutrient and sediment transfer in catchments. Sci. Total Environ. 543, 388–404.
Maringanti, C., Chaubey, I., Popp, J., 2009. Development of a multiobjective optimization tool for the selection and placement of best management practices for nonpoint source pollution control. Water Resour. Res. 45 https://doi.org/10.1029/2008WR007094.
McDonnell, J.J., Beven, K., 2014. Debates-The future of hydrological sciences: A (common) path forward? A call to action aimed at understanding velocities, celerities and residence time distributions of the headwater hydrograph. Water Resour. Res. 50, 5342–5350.
McMillan, H., Tetzlaff, D., Clark, M., Soulsby, C., 2012. Do time-variable tracers aid the evaluation of hydrological model structure? A multimodel approach. Water Resour. Res. 48 https://doi.org/10.1029/2011WR011688.

Musolff, A., Schmidt, C., Selle, B., Fleckenstein, J.H., 2015. Catchment controls on solute export. Adv. Water Resour. 86, 133–146.
Musolff, A., Fleckenstein, J.H., Rao, P.S.C., Jawitz, J.W., 2017. Emergent archetype patterns of coupled hydrologic and biogeochemical responses in catchments. Geophys. Res. Lett. 44, 4143–4151.
Perks, M.T., Owen, G.J., Benskin, C.M.H., Jonczyk, J., Deasy, C., Burke, S., Reaney, S.M., Haygarth, P.M., 2015. Dominant mechanisms for the delivery of fine sediment and phosphorus to fluvial networks draining grassland dominated headwater catchments. Sci. Total Environ. 523, 178–190.
Piovano, T.I., Tetzlaff, D., Carey, S.K., Shatilla, N.J., Smith, A., Soulsby, C., 2019. Spatially distributed tracer-aided runoff modelling and dynamics of storage and water ages in a permafrost-influenced catchment. Hydrol. Earth Syst. Sci. 23, 2507–2523.
Reddy, K.R., Newman, S., Osborne, T.Z., White, J.R., Fitz, H.C., 2011. Phosphorous Cycling in the Greater Everglades Ecosystem: Legacy Phosphorous Implications for Management and Restoration. Crit. Rev. Environ. Sci. Technol. 41, 149–186.
Remondi, F., Kirchner, J.W., Burlando, P., Fatichi, S., 2018. Water Flux Tracking With a Distributed Hydrological Model to Quantify Controls on the Spatiotemporal Variability of Transit Time Distributions. Water Resour. Res. 54, 3081–3099.
Rinaldo, A., Benettin, P., Harman, C.J., Hrachowitz, M., McGuire, K.J., van der Velde, Y., Bertuzzo, E., Botter, G., 2015. Storage selection functions: A coherent framework for quantifying how catchments store and release water and solutes. Water Resour. Res. 51, 4840–4847.
Schilling, K.E., Helmers, M., 2008. Tile drainage as karst: Conduit flow and diffuse flow in a tile-drained watershed. J. Hydrol. 349, 291–301.
Schwab, M.P., Klaus, J., Pfister, L., Weiler, M., 2017. How runoff components affect the export of DOC and nitrate: a long-term and high-frequency analysis. Earth Syst. Sci Hydrol. https://doi.org/10.5194/hess-2017-416.
Soulsby, C., Birkel, C., Geris, J., Dick, J., Tunaley, C., Tetzlaff, D., 2015. Stream water age distributions controlled by storage dynamics and nonlinear hydrologic connectivity: Modeling with high-resolution isotope data. Water Resour. Res. 51, 7759–7776.
Sprenger, M., Stumpp, C., Weiler, M., Aeschbach, W., Allen, S.T., Benettin, P., Dubbert, M., Hartmann, A., Hrachowitz, M., Kirchner, J.W., McDonnell, J.J., Orlowski, N., Penna, D., Pfahl, S., Rinderer, M., Rodriguez, N., Schmidt, M., Werner, C., 2019. The Demographics of Water: A Review of Water Ages in the Critical Zone. Rev. Geophys. 57, 800–834.
Tesoriero, A.J., Puckett, L.J., 2011. O 2 reduction and denitrification rates in shallow aquifers. Water Resour. Res. 47 https://doi.org/10.1029/2011WR010471.
Tetzlaff, D., Birkel, C., Dick, J., Geris, J., Soulsby, C., 2014. Storage dynamics in hydropedological units control hillslope connectivity, runoff generation, and the evolution of catchment transit time distributions. Water Resour. Res. 50, 969–985.
Tihansky, A.B., 1999. Sinkholes, west-central Florida: A link between surface water and ground water, in Galloway, D., Jones, D.R., and Ingebritsen, S.E., eds.,. L. Subsid. United States US Geol. Surv. Circ. 1182, 121–140.
Tunaley, C., Tetzlaff, D., Lessels, J., Soulsby, C., 2016. Linking high-frequency DOC dynamics to the age of connected water sources. Water Resour. Res. 52, 5232–5247.
van Schaik, N.L.M.B., Schnabel, S., Jetten, V.G., 2008. The influence of preferential flow on hillslope hydrology in a semi-arid watershed (in the Spanish Dehesas). Hydrol. Process. 22, 3844–3855.
Wang, Z.-J., Li, S.-L., Yue, F.-J., Qin, C.-Q., Buckerfield, S., Zeng, J., 2020. Rainfall driven nitrate transport in agricultural karst surface river system: Insight from high resolution hydrochemistry and nitrate isotopes. Agric. Ecosyst. Environ. 291, 106787.
White, W.B., 2002. Karst hydrology: recent developments and open questions. Eng. Geol. 65, 85–105.
Yang, P., Wang, Y., Wu, X., Chang, L., Ham, B., Song, L., Groves, C., 2020. Nitrate sources and biogeochemical processes in karst underground rivers impacted by different anthropogenic input characteristics. Environ. Pollut. 265, 114835.
Yue, F.-J., Li, S.-L., Liu, C.-Q., Lang, Y.-C., Ding, H., 2015. Sources and transport of nitrate constrained by the isotopic technique in a karst catchment: an example from Southwest China. Hydrol. Process. 29, 1883–1893.
Yue, F.-J., Li, S.-L., Waldron, S., Wang, Z.-J., Oliver, D.M., Chen, X., Liu, C.-Q., 2020. Rainfall and conduit drainage combine to accelerate nitrate loss from a karst agroecosystem: insights from stable isotope tracing and high-frequency nitrate sensing. Water Res. https://doi.org/10.1016/j.watres.2020.116388.
Yue, F.-J., Waldron, S., Li, S.-L., Wang, Z.-J., Zeng, J., Xu, S., Zhang, Z.-C., Oliver, D.M., 2019. Land use interacts with changes in catchment hydrology to generate chronic nitrate pollution in karst waters and strong seasonality in excess nitrate export. Sci. Total Environ. 696, 134062.
Zhang, Z., Chen, X., Cheng, Q., Soulsby, C., 2019. Storage dynamics, hydrological connectivity and flux ages in a karst catchment: conceptual modelling using stable isotopes. Hydrol. Earth Syst. Sci. 23, 51–71.
Zhang, Z., Chen, X., Ghadouani, A., Shi, P., 2011. Modelling hydrological processes influenced by soil, rock and vegetation in a small karst basin of southwest China. Hydrol. Process. 25, 2456–2470.
Zhang, Z., Chen, X.i., Chen, X., Shi, P., 2013. Quantifying time lag of epikarst-spring hydrograph response to rainfall using correlation and spectral analyses. Hydrogeol. J. 21, 1619–1631.
Zhang, Z., Chen, X., Cheng, Q., Li, S., Yue, F., Peng, T., Waldron, S., Oliver, D.M., Soulsby, C., 2020a. Coupled hydrological and biogeochemical modelling of nitrogen transport in the karst critical zone. Sci. Total Environ. 732, 138902.
Zhang, Z., Chen, X., Cheng, Q., Soulsby, C., 2020b. Characterizing the variability of transit time distributions and young water fractions in karst catchments using flux tracking. Hydrol. Process. 34, 3156–3174.
Zhi, W., Li, L., Dong, W., Brown, W., Kaye, J., Steefel, C., Williams, K.H., 2019. Distinct Source Water Chemistry Shapes Contrasting Concentration-Discharge Patterns. Water Resour. Res. 55, 4233–4251.